JACC: BASIC TO TRANSLATIONAL SCIENCE VOL. 4, NO. 2, 2019

PRECLINICAL RESEARCH

Phosphorylation of Hsp20 Promotes Fibrotic Remodeling and Heart Failure

George T. Gardner, PhD,[a] Joshua G. Travers, PhD,[b] Jiang Qian, PhD,[a] Guan-Sheng Liu, PhD,[a] Kobra Haghighi, PhD,[a] Nathan Robbins, MS,[c] Min Jiang, BS,[c] Yutian Li, MS,[a] Guo-Chang Fan, PhD,[a] Jack Rubinstein, MD,[c] Burns C. Blaxall, PhD,[b] Evangelia G. Kranias, PhD[a,d]

VISUAL ABSTRACT

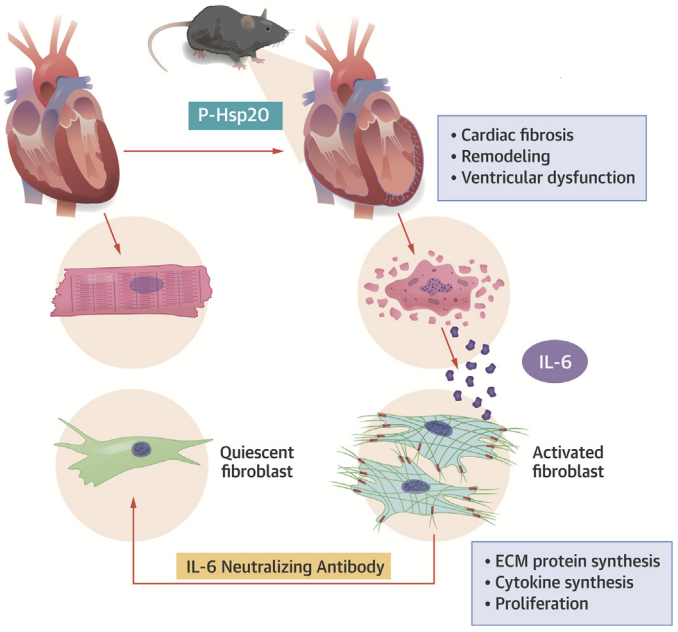

Gardner, G.T. et al. J Am Coll Cardiol Basic Trans Science. 2019;4(2):188–99.

HIGHLIGHTS

- **PKA-phosphorylation of Hsp20 is elevated in human failing hearts.**
- **Increases in phosphorylated Hsp20 in vivo are associated with fibrotic remodeling and reduced left ventricular function.**
- **The phosphorylated Hsp20 in cardiomyocyte promotes upregulation of IL-6 and its subsequent paracrine actions on the cardiac fibroblast.**
- **Blockade of IL-6 effects ex vivo and in vivo reduces the pro-fibrotic effects of phosphorylated Hsp20.**
- **Targeting phosphorylated Hsp20 in the cardiomyocyte may represent a potential therapeutic strategy to mitigate fibrotic remodeling and preserve function in the failing heart.**

From the [a]Department of Pharmacology and Systems Physiology, University of Cincinnati College of Medicine, Cincinnati, Ohio; [b]Department of Pediatrics, Division of Molecular Cardiovascular Biology, The Heart Institute, Cincinnati Children's Hospital Medical Center, Cincinnati, Ohio; [c]Department of Internal Medicine, University of Cincinnati College of Medicine, Cincinnati, Ohio; and the [d]Molecular Biology Division, Center for Basic Research, Biomedical Research Foundation of the Academy of Athens, Athens, Greece. This research was supported by U.S. National Institutes of Health (NIH) grants R01 HL26057, R01 HL64018 (EGK), R01 HL132551, R01 HL133695, R01 HL134321 to Dr. Blaxall; and predoctoral fellowship grants 15PRE25090055 and NIH grant T32 HL125204 from the American Heart Association Great Rivers Affiliate to Dr. Gardner. All other authors have reported that they have no relationships relevant to the contents of this paper to disclose.

All authors attest they are in compliance with human studies committees and animal welfare regulations of the authors' institutions and U.S. Food and Drug Administration guidelines, including patient consent where appropriate. For more information, visit the *JACC: Basic to Translational Science* author instructions page.

Manuscript received August 22, 2018; revised manuscript received September 27, 2018, accepted November 14, 2018.

ISSN 2452-302X https://doi.org/10.1016/j.jacbts.2018.11.007

SUMMARY

Cardiomyocyte-specific increases in phosphorylated Hsp20 (S16D-Hsp20) to levels similar to those observed in human failing hearts are associated with early fibrotic remodeling and depressed left ventricular function, symptoms which progress to heart failure and early death. The underlying mechanisms appear to involve translocation of phosphorylated Hsp20 to the nucleus and upregulation of interleukin (IL)-6, which subsequently activates cardiac fibroblasts in a paracrine fashion through transcription factor STAT3 signaling. Accordingly, treatment of S16D-Hsp20 mice with a rat anti-mouse IL-6 receptor monoclonal antibody (MR16-1) attenuated interstitial fibrosis and preserved cardiac function. These findings suggest that phosphorylated Hsp20 may be a potential therapeutic target in heart failure. (J Am Coll Cardiol Basic Trans Science 2019;4:188–99)

ABBREVIATIONS AND ACRONYMS

Ccl2 = C-C motif chemokine ligand 2

Ccl3 = C-C motif chemokine ligand 3

Col1a1 = collagen 1A1

Col3A1 = collagen 3A1

ECM = extra-cellular matrix

Hsp = heat shock protein

I/R = ischemia/reperfusion

IL = interleukin

Postn = periostin

SMA = smooth muscle actin

STAT3 = signal transducer and activator of transcription 3

TG = transgenic

TGF = transforming growth factor

TNF = tumor necrosis factor

TUNEL = terminal deoxynucleotidyl transferase dUTP nick end labeling

WT = wild type

Heart failure is a world-wide health problem affecting approximately 26 million people (1). Although significant advances have been made in the management of disease symptoms, morbidity and mortality rates remain high throughout the world (1). Studies aiming to understand the mechanisms, the underlying causes, and the progression of heart failure have implicated several signaling pathways. Specifically, the β-adrenergic axis, including its downstream regulatory phosphorylation substrates, has been shown to play a major role in cardiac remodeling (2). However, it is puzzling that some cyclic adenosine monophosphate-dependent phosphoproteins are downregulated, whereas others are increased in failing hearts (3). These altered responses may reflect the fine balance between protein kinase and phosphatase activities in subcellular compartments during heart failure progression (4). Among the cardiac phosphoproteins in the β-adrenergic transduction pathway is the small heat shock protein 20 (Hsp20 or HspB6), which has recently drawn particular attention.

SEE PAGE 200

Hsp20 belongs to the subfamily Hsps, which consists of 10 members whose molecular masses range from 12 to 43 kDa (5). It is a highly conserved protein and can be detected in all tissues but is most abundant in cardiac, skeletal, and smooth muscles (6). The levels of Hsp20 are mostly upregulated in human failing hearts (7) and in animal models upon oxidative stress, ischemia-reperfusion (I/R) injury, exercise training, and chronic β-adrenergic stimulation (8). These findings suggest that Hsp20 may play a critical role in cellular stress resistance as an adaptive response after exposure to stress stimuli. Indeed, adenoviral studies and studies in transgenic (TG) mice with cardiac-specific increases in Hsp20 have demonstrated a protective role for this protein against β-agonist-induced apoptosis (9,10), chronic doxorubicin-induced oxidative stress (11), and I/R injury (12).

Hsp20 was initially discovered as a phosphoprotein induced upon prolonged β-adrenergic stimulation of cardiomyocytes (13). Proteomic analysis revealed that phosphorylation occurs at Ser16 by protein kinase A, a phenomenon unique to Hsp20 among the small Hsp family (13). Subsequent investigations have shown that phosphorylation at Ser16 was elevated in human failing hearts as well as in murine hearts after I/R injury (7,12), suggesting that Hsp20 may function as an innate protector. Indeed, studies from the present authors' laboratory have indicated that overexpression of a constitutively phosphorylated form of Hsp20 (S16D) in cultured cardiomyocytes conferred protection against isoproterenol-induced cellular apoptosis, whereas overexpression of constitutively dephosphorylated Hsp20 (S16A) offered no anti-apoptotic benefits (9). Moreover, TG mice with cardiac-specific overexpression of the dephosphorylated S16A-Hsp20 exhibited diminished functional recovery and greater infarct size following I/R injury, both of which were associated with increased cardiomyocyte necrosis and apoptosis (7). These findings implicated phosphorylation of Hsp20 as a potential cardioprotector.

The critical role of Hsp20 in the heart and the potential benefits of its phosphorylation prompted examination of the functional significance and long-term effects of Hsp20 phosphorylation at Ser16 in vivo. To this end, the present authors generated a model with cardiac-specific overexpression of a constitutively phosphorylated Hsp20 form (S16D-Hsp20) and chose a mouse line with levels similar to those observed in human failing hearts for

characterization (7). Surprisingly, and in contrast to previous findings, S16D-Hsp20 mice exhibited early fibrotic remodeling and dysfunction, which progressed to the development of heart failure. Ex vivo studies have revealed that these effects were linked to the pro-fibrotic role of phosphorylated Hsp20, which induced synthesis of interleukin (IL)-6 in cardiomyocytes and its subsequent paracrine activation of cardiac fibroblasts through transcription factor STAT3 signaling. Accordingly, treatment of S16D mice using a rat anti-mouse IL-6 receptor monoclonal antibody (MR16-1) attenuated interstitial fibrosis and preserved left ventricular (LV) function. Taken together, these results reveal a novel functional role for Hsp20 in the heart and indicate that increases in Hsp20 phosphorylation appear to be maladaptive and may exacerbate the progression to heart failure.

METHODS

Additional detailed methods are available in the Supplemental Appendix.

EXPERIMENTAL MODELS. All animal procedures were performed according to guidelines set forth by the U.S. National Institutes of Health and those of the Institutional Animal Care and Use Committee at the University of Cincinnati. TG mice with cardiac-specific overexpression of constitutively phosphorylated Hsp20 (S16D-Hsp20) were generated as previously described (7) and carried the mouse cardiac S16D-Hsp20 cDNA under the control of the α-myosin heavy chain promoter. Male TG and wild-type (WT) age-matched control mice were used for all studies. For endpoint studies, mouse hearts were excised following anesthesia (200 mg/kg intraperitoneally [IP], Euthasol, Virbac AH, Inc., Fort Worth, Texas) and used for further analysis.

CARDIOMYOCYTE AND CARDIAC FIBROBLAST CROSS-TALK EXPERIMENTAL DESIGN. Cardiomyocyte and cardiac fibroblast isolation procedures were performed as described in the Supplemental Methods. Following cardiomyocyte isolation, the cardiomyocyte pellet was resuspended in a solution of plating medium (Dulbecco's modified Eagle medium [DMEM]), 10% fetal bovine serum [FBS], and 1% penicillin-streptomycin [Pen/Strep, ThermoFisher Scientific, Waltham, Massachusetts] plus 0.2% 2,3-butanedione monoxime), which was plated on laminin-coated dishes and incubated for 1 h at 37°C. The medium was replaced with infection medium (plating medium with no FBS), and cardiomyocytes were infected with adenovirus-infected green fluorescent protein (Ad.GFP), and with Ad.S16D or adenovirus-infected constitutively dephosphorylated Hsp20A (Ad.S16A) at a multiplicity of infection of 100. After 2 h of infection, the cells were transferred to culture medium consisting of a solution of DMEM plus 5 mg/l insulin-transferrin-selenium (Sigma-Aldrich, St. Louis, Missouri), 100 U/ml penicillin/streptomycin, 2 mM of L-glutamine, 4 mM $NaHCO_3$, 10 mM Hepes, 0.2% bovine serum albumin, and 25 μM blebbistatin (Cayman Chemical, Ann Arbor, Michigan) for 48 h. Medium was replaced after 24 h, after which the cardiomyocytes were collected for protein and RNA isolation. The conditioned medium was obtained and centrifuged at 5,000 *g* for 10 min to remove cell debris and stored at −80°C.

The ventricular fibroblasts were plated in growth medium and allowed to grow for 4 to 5 days until confluent. After fibroblasts were passaged in dishes appropriately sized for subsequent experiments, they were cultured in growth medium containing the cardiomyocyte-conditioned medium at a dilution of 1:1. Fibroblast proliferation was determined by using the MTT cell growth assay (catalog number CT02, MilliporeSigma, Burlington, Massachusetts) as previously described (14). Gene expression of pro-fibrotic markers was assessed using quantitative polymerase chain reaction (qPCR), and alpha-smooth muscle actin (SMA) stress fiber formation was evaluated using immunofluorescence. IL-6 inhibition was achieved through addition of an IL-6-neutralizing antibody (catalog number MAB406, R & D Systems, Minneapolis, Minnesota) to the conditioned medium upon application to the fibroblasts at a concentration of 0.60 μg/ml, based on a previously established protocol (15).

MR16-1 TREATMENT. Four-week old male S16D and WT control mice were injected with the rat anti-mouse IL-6 receptor monoclonal antibody MR16-1 (Genentech, San Francisco, California), as described later, using previously established protocols with minor modifications (16,17). Echocardiography was performed before the first injection and subsequently at 2 and 4 weeks afterward. Immediately after baseline echocardiography was performed, mice were given 2 mg/body MR16-1 or phosphate-buffered saline (PBS) as control by IP injection. During the first, second, and third weeks after the initial injection, mice received 0.5 mg/week MR16-1 or PBS (0.25 mg/body × 2 injections/week). At 8 weeks of age, following the final echocardiographic assessment, mice were sacrificed, and hearts were removed for examination of fibrosis using PicroSirius Red staining (Abcam, Cambridge, Massachusetts). Cardiac fibroblasts and

FIGURE 1 S16D-Hsp20 Transgenic Mice Exhibit Reduced Survival, Left Ventricular Remodeling, and Dysfunction

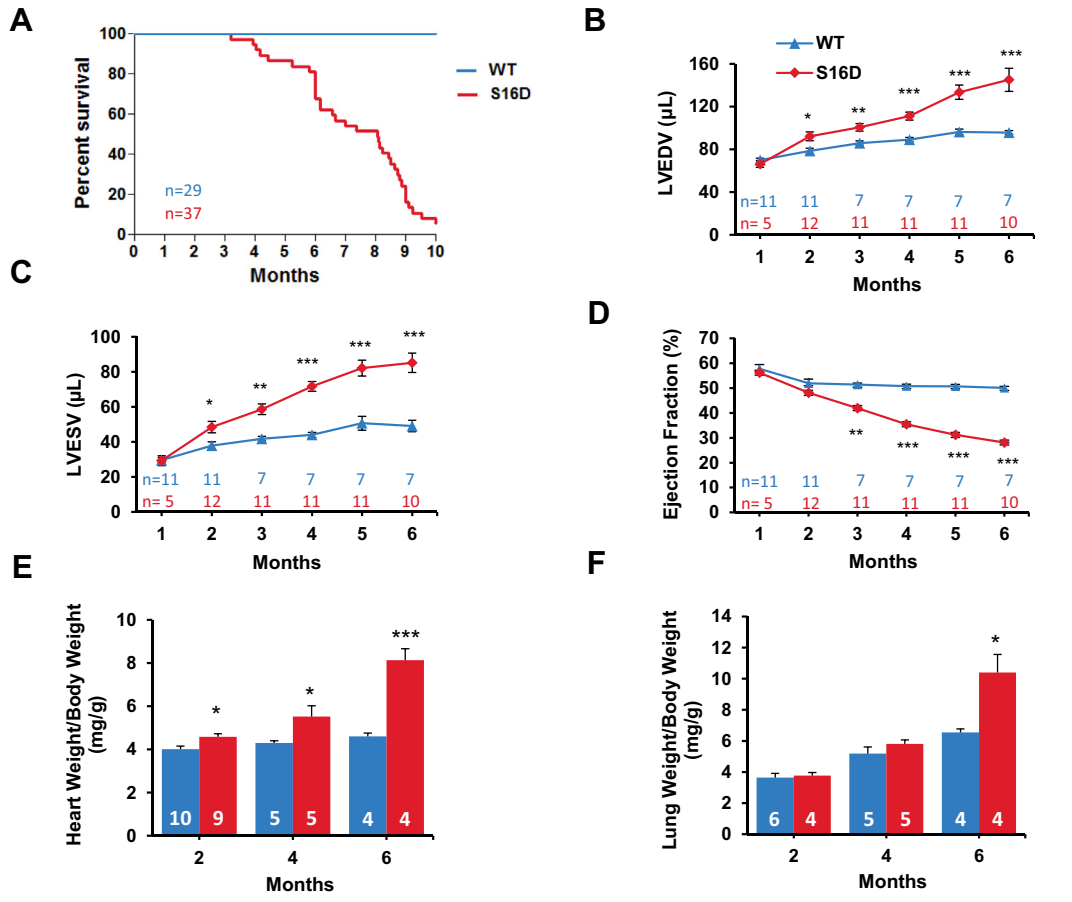

(A) Kaplan-Meier survival curve of S16D and WT control mice. Longitudinal echocardiographic assessment of S16D and WT mice at 2, 4, and 6 months of age: **(B)** LVEDV; **(C)** LVESV; and **(D)** EF. Gravimetric analysis of S16D and WT control mice at 2, 4, and 6 months of age. Ratios of **(E)** heart weight/body weight and **(F)** lung weight/body weight in S16D and WT control mice. Values are mean ± SEM. *$p < 0.05$; **$p < 0.01$; ***$p < 0.001$ versus WT. The number of samples (n) per group is indicated on the bar graphs. EF = ejection fraction; LVEDV = left ventricular end diastolic volume; LVESV = left ventricular end systolic volume; S16D = phosphorylated Hsp20; WT = wild type.

cardiomyocytes were isolated from a second cohort of treated and nontreated WT and S16D mice, as described in the Supplemental Methods. STAT3 signaling was assessed in the isolated fibroblasts by Western blotting, and expression of remodeling markers (*ANP*, *BNP*, and *β-MHC*) were measured using qPCR.

STATISTICS. Data were expressed as mean ± SEM. Comparisons between the means of 2 groups were evaluated using an unpaired Student *t*-test at each time point (**Figures 1B to 1F and 2D**) or the Mann-Whitney *U* test for data sets shown in **Figure 2B**, due to the small sample size (n = 3). Comparisons of more than 2 groups were performed using 1-way analysis of variance (ANOVA) followed by the Tukey multiple comparison test (**Figures 3B to 3E and 5F**). Alternatively, the Kruskal-Wallis test followed by Dunn's multiple comparison test was used for data shown in **Figure 5H**, due to the small sample size (n = 3). Groups which originated from the same heart were compared using a paired Student *t*-test (**Figure 4B**) or 1-way repeated measures ANOVA, followed by Tukey's multiple comparison test (**Figure 3A**). Data in **Figure 3G** were analyzed by using the Friedman test followed by Dunn's multiple comparison test, because of the small sample size (n = 3). Comparisons among the expression levels of 4 genes in the adenovirus-infected cardiomyocytes (**Figure 4A**) were performed by 2-way repeated measures ANOVA, followed by Bonferroni correction. Comparisons among groups in the MR16-1 treatment study (**Figure 5D**) were performed using 2-way repeated measures ANOVA, followed by the Neuman-Keuls multiple

FIGURE 2 Extensive Interstitial Fibrosis Evident in S16D-Hsp20 Hearts

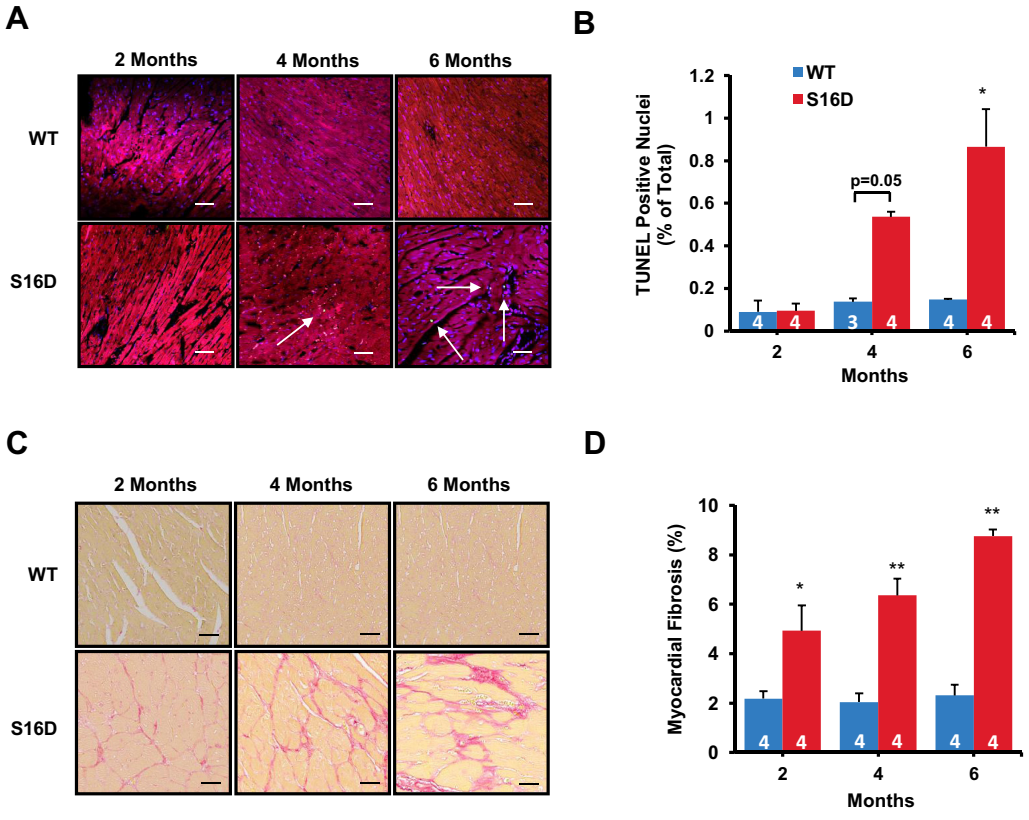

(A) Representative confocal images (original magnification: ×20) for TUNEL staining **(green)** counterstained with actin **(red)** and DAPI to visualize nuclei **(blue)**. **Arrows** indicate TUNEL-positive cells; scale bar: 50 μm. **(B)** Quantitative analysis of TUNEL-positive nuclei (expressed as a percentage of total nuclei) in S16D and WT ventricular sections at 2, 4, and 6 months of age. **(C)** Representative images (original magnification: ×20) of ventricular sections stained with Picrosirius red; scale bar: 50 μm. **(D)** Quantitative analysis of ventricular fibrosis (expressed as a percentage of total area) in S16D and WT hearts at 2, 4, and 6 months of age. The number of samples (n) per group is indicated on the bar graphs. DAPI = 4′,6-diamidino-2-phenylindole; TUNEL = terminal deoxynucleotidyl transferase dUTP nick end labeling; other abbreviations as in Figure 1.

comparison test. Analysis of survival was performed using the Kaplan-Meier method (using 29 WT control and 37 S16D mice). The following statistical thresholds were applied: $p < 0.05$, $p < 0.01$, and $p < 0.001$. Comparisons were made among the experimental groups and WT or GFP or among the indicated groups. Statistical analyses were performed using Prism version 8 software (GraphPad, San Diego, California).

RESULTS

S16D-Hsp20 TRANSGENIC MICE EXHIBITED CARDIAC REMODELING, DYSFUNCTION, AND EARLY MORTALITY. Hsp20 is upregulated and hyperphosphorylated in human heart failure and experimental I/R injury (7,12). To determine the functional significance of increases in Hsp20 phosphorylation, TG mice with cardiac-specific overexpression of a constitutively phosphorylated mutation (S16D-Hsp20) were generated (Supplemental Figure S1A). A TG mouse line was chosen that expressed increases in S16D-Hsp20 levels similar to those observed in human failing hearts (7) (Supplemental Figures S1B and S1C) for further characterization studies. Interestingly, S16D mice exhibited significantly reduced survival, with a mortality rate of approximately 50% by 7 months and 100% by 10 months of age (Figure 1A). There were no parallel deaths in either WT (Figure 1A) or TG mice with similar levels of WT-Hsp20 overexpression (12). Longitudinal assessment of LV geometry using echocardiography indicated significant chamber

FIGURE 3 S16D-Hsp20 Cardiomyocyte-Conditioned Medium Activates Myofibroblast Differentiation

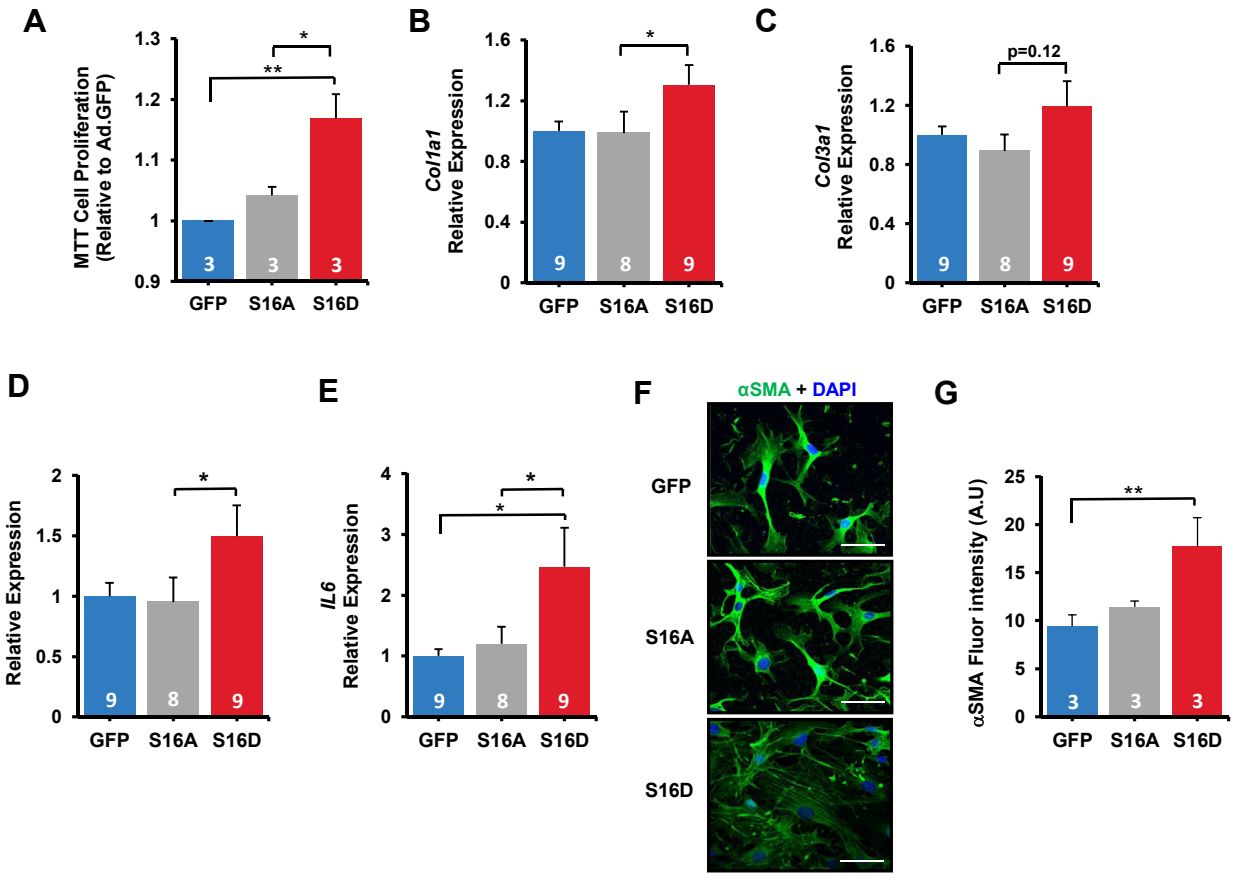

Adult mouse cardiac fibroblasts were cultured in conditioned medium from Ad.GFP, Ad.S16D, Ad.S16A. Fibroblast proliferation and markers of myofibroblast differentiation were assessed. **(A)** Quantification of fibroblast proliferation was determined using the MTT assay. Values are fold changes relative to those of Ad.GFP. Relative gene expression levels are shown for **(B)** *Col1a1*; **(C)** *Col3a1*; **(D)** *TGFβ1*; and **(E)** *IL-6*. Values are fold-changes relative to those of Ad.GFP. **(F)** Representative confocal images (original magnification: ×40) of fibroblasts stained with αSMA **(green)** plus DAPI to visualize nuclei **(blue)**; scale bar: 50 μm. **(G)** Quantification of αSMA fluorescence intensity. The number of samples (n) per group is indicated on the bar graphs. SMA = smooth muscle actin; Ad.GFP = adenovirus-infected green fluorescent protein; Ad.S16D = adenovirus-infected phosphorylated Hsp16D; Ad.S16A = adenovirus-infected dephosphorylated Hsp16A; *Col1a1* = collagen 1a1; *Col3a1* = collagen 3a1; *IL* = interlukin-6; *TGF* = transforming growth factor; other abbreviations as in Figure 2.

dilation (i.e., LV end-diastolic volume and LV end-systolic volume) in S16D mice, which became evident as early as 2 months of age (Figures 1B and 1C). These geometrical alterations were accompanied by a decrease in ejection fraction (EF) by 3 months of age (Figure 1D). The EF continued to deteriorate over time to <50% of normal by 6 months, concomitant with 50% mortality (Figure 1D). In contrast, TG mice overexpressing nonphosphorylated Hsp20 (S16A) at levels similar to those of S16D-Hsp20 mice did not exhibit any alterations in LV function and geometry up to 6 months of age (Supplemental Figure S2A to S2C). Further morphological, histological, and cellular studies were concentrated at the following 3 time points: at 2 months of age, at which point no change in LV function and slight chamber dilation occurred; at 4 months of age, when a significant decline in LV function and chamber dilation were exhibited but minimal deaths; and at 6 months, when severe dysfunction, extensive chamber dilation, and close to 50% mortality occurred (Figure 1A). Gravimetric analysis revealed a 13% increase in heart weight/body weight ratio as early as 2 months, which further increased at 4 and 6 months in S16D mice compared to those in WT mice (Figure 1E). Accordingly, cardiomyocyte hypertrophy, determined by wheat germ agglutinin staining, was increased at 2 months and was further augmented at 4 and 6 months

FIGURE 4 Acute Overexpression of S16D-Hsp20 in Cardiomyocytes Promotes Upregulation of the *IL-6* Gene Expression and Secretion

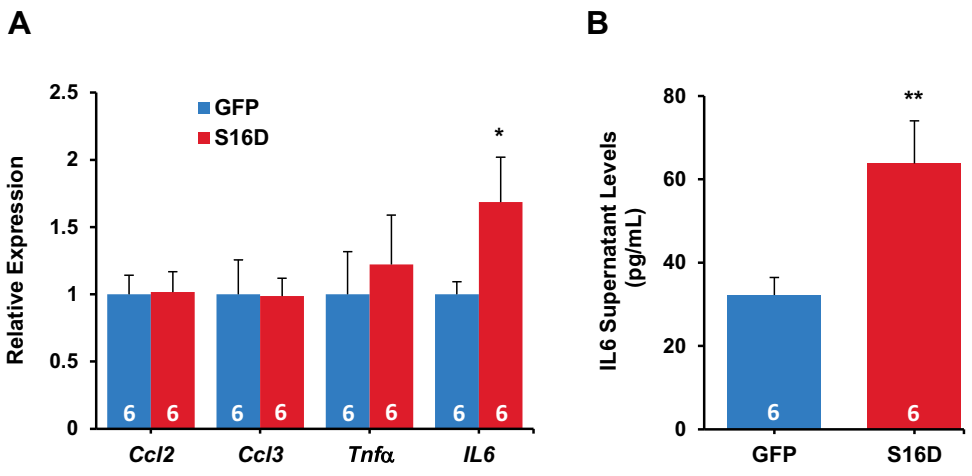

(A) Assessment of the following cytokine gene expression levels in Ad.GFP and Ad.S16D cardiomyocytes *Ccl2*, *Ccl3*, *TNF-α*, and *IL-6*. *TGFβ1* and *IL-1β* were not detectable in either group. Values were normalized to those of the internal control, 18 S, and expressed as fold-changes relative to those of Ad.GFP. **(B)** Quantification of IL-6 secretion into the conditioned medium from Ad.GFP and Ad.S16D cardiomyocytes was determined by using an ELISA assay. The number of samples (n) per group is indicated on the bar graphs. *Ccl2* = C-C motif chemokine ligand 2; *Ccl3* = C-C motif chemokine ligand 3; ELISA = enzyme-linked immunosorbent assay; MR16-1 = rat anti-mouse IL-6 receptor monoclonal antibody; *TNF* = tumor necrosis factor; WT = wild type; other abbreviations as in Figure 3.

(Supplemental Figures S3A and S3B). Analysis of gene expression of remodeling markers indicated that only the atrial natriuretic peptide (*ANP*) level was significantly elevated at 2 months of age. However, by 6 months of age, *ANP*, brain natriuretic peptide (*BNP*), and β-myosin heavy chain (*MHC*) levels were all significantly increased in S16D hearts (Supplemental Figure S3). Assessment of lung congestion indicated significant increases only at 6 months of age in S16D mice (**Figure 1F**). These results suggested that cardiac overexpression of S16D promoted early LV dilation, culminating in cardiac dysfunction and development of heart failure, resulting in early death.

EARLY INTERSTITIAL FIBROSIS. Evidence indicates that the advancement of cardiac remodeling is associated with myocyte apoptosis and interstitial fibrosis (18). Thus, cardiomyocyte loss in S16D hearts was assessed by terminal deoxynucleotidyl transferase dUTP nick end labeling (TUNEL) assay. There were significant levels of apoptosis at 4 and 6 months compared to WT control mice, whereas there was no evidence of TUNEL-positive nuclei at 2 months (**Figures 2A and 2B**). The absence of cardiomyocyte death at 2 months was further confirmed by lack of alterations in serum levels of cardiac troponin I (Supplemental Figure S4A) as well as caspase-3 activity (Supplemental Figure S4B) and the apoptotic markers Bak, Bcl-2, and Bax (Supplemental Figures S4C and S4D). Surprisingly, although there was no evidence of cell death at 2 months, significant interstitial fibrosis was observed by PicroSirius Red (Abcam) staining (**Figures 2C and 2D**). Collagen deposition was further determined through assessment of hydroxyproline content in S16D hearts. This assessment demonstrated a significant increase at 2 months, which was further increased at 6 months of age (Supplemental Figure S5A). These increases were accompanied by significant upregulation of the profibrotic markers collagen 1A1 (*Col1a1*) and transforming growth factor *(TGF)-β1* and by a trend toward increased expression of periostin (*Postn*) (Supplemental Figures S5B to S5D). Collectively, the data suggest that S16D-Hsp20 promotes early interstitial fibrosis in the absence of cardiomyocyte death in the heart.

CROSSTALK BETWEEN S16D CARDIOMYOCYTES AND FIBROBLASTS. Cardiac fibroblasts are responsible for extracellular matrix homeostasis, providing structural support for cardiomyocytes (18,19). Upon pathological stimulation, fibroblasts transition to the myofibroblast phenotype, which can promote excessive collagen secretion, leading to pathological remodeling (19). Recent studies have identified-dynamic crosstalk between cardiomyocytes and

fibroblasts, which occurs through secreted factors (20–22). Thus, these authors sought to determine whether S16D overexpression in the cardiomyocytes promote myofibroblast transition through a paracrine mechanism. To this end, isolated ventricular cardiomyocytes and fibroblasts from adult mouse hearts were used and with the cardiomyocytes were Ad.GFP and Ad.S16D or the constitutively dephosphorylated Hsp20, Ad.S16A, as an additional control. The Hsp20 overexpression levels in S16D and S16A cardiomyocytes were similar (Supplemental Figures S6A and S6B). Then, the conditioned medium from the infected cardiomyocytes was used to culture fibroblasts, and their potential activation was assessed using key markers (19). Fibroblasts in the S16D medium exhibited significantly enhanced proliferation (**Figure 3A**) and significant upregulation of *Col1a1*, *(TGF)-β1*, and *IL-6*, as well as a trend toward upregulation of collagen 3A1 (*Col13a1*) (**Figures 3B to 3E**). Further analysis using immunofluorescence revealed the presence of prominent αSMA-positive stress fibers in S16D fibroblasts (**Figures 3F and 3G**), a reliable indicator of myofibroblast activation in culture. Importantly, the effects observed on fibroblast differentiation were specific to S16D as there were no alterations elicited by the S16A medium (**Figures 3A to 3G**). To exclude cardiomyocyte death as a contributing factor to fibroblast activation (22), the levels of lactate dehydrogenase were determined in the conditioned medium. There were no differences in the levels of lactate dehydrogenase released among the 3 groups (Supplemental Figure S6C). These findings demonstrate that overexpression of S16D in the cardiomyocytes may promote the secretion of a factor(s) which stimulates differentiation of fibroblasts to myofibroblasts.

IL-6 IS UPREGULATED IN S16D CARDIOMYOCYTES. The findings described above coupled with previous evidence indicating that secretion of cytokines from the cardiomyocyte (23) can activate myofibroblast differentiation (24) prompted an examination of the expression levels of C-C motif chemokine ligand 2 (*Ccl2)*, C-C motif chemokine ligand 3 (*Ccl3*), *IL-6*, tumor necrosis factor *(TNF)-α, TGFβ1*, and *IL-1β* in Ad.S16D cardiomyocytes. Interestingly, only IL-6 expression was upregulated (**Figure 4A**), and this upregulation was associated with its increased secretion into the medium from the cardiomyocytes (**Figure 4B**). Taken together, these data indicate that increases in S16D in cardiomyocytes promote IL-6 transcriptional upregulation and its subsequent secretion to the extracellular space.

BLOCKING IL-6 REDUCES PRO-FIBROTIC EFFECTS OF S16D. To determine the role of IL-6 in the pro-fibrotic effects elicited by the S16D cardiomyocytes, an IL-6-neutralizing antibody, M16-1, was included in the conditioned medium that was applied to fibroblasts. There was a reduction in the expression levels of collagens and cytokines in the fibroblasts treated with the IL-6 antibody, although statistical significance was not reached (Supplemental Figures S6D and S7A). Furthermore, αSMA stress fiber formation was abrogated in the presence of the IL-6 antibody (Supplemental Figures S7E and S7F). To further confirm the role of IL-6 in the transition of fibroblasts to myofibroblasts, the question of whether STAT3 localized to the nucleus was examined, as its phosphorylation and nuclear translocation occurred upon stimulation of the IL-6 receptor (IL-6R) (25). Indeed, nuclear accumulation of phosphorylated STAT3 (P-STAT3) was significantly greater in fibroblasts treated with the S16D medium (Supplemental Figure S7G). Accordingly, inclusion of the IL-6 antibody abrogated this effect (Supplemental Figure S7G). These results suggested that S16D overexpression in the cardiomyocyte promotes myofibroblast differentiation through a paracrine mechanism by activation of the IL-6/STAT3 signaling pathway in the fibroblast.

TREATMENT OF S16D MICE WITH MR16-1 ATTENUATED FIBROSIS AND IMPROVED CARDIAC FUNCTION. Our ex vivo findings led to an investigation of whether IL-6 was contributing to the excessive collagen deposition and cardiac remodeling in the S16D mice, which was observed as early as 2 months of age. Indeed, both cardiac and serum IL-6 levels were higher in S16D mice than in WT mice (**Figures 5A and 5B**). Because IL-6 has been implicated in fibrotic ventricular remodeling (26), the authors hypothesized that treatment of S16D mice with an IL-6 receptor antagonist (MR16-1) would reduce ventricular fibrosis and preserve function. Therefore, S16D and WT mice were treated with MR16-1 or PBS for 4 weeks, starting at 1 month of age, when no ventricular dysfunction or remodeling was evident (**Figure 5C**). Treatment with MR16-1 prevented deterioration of function (EF) in S16D mice (**Figure 5D**), although it had no effects on ventricular chamber dilation, cardiomyocyte hypertrophy, or remodeling markers (Supplemental Figures S8A to S8F), indicating that a separate mechanism might have been contributing to remodeling in S16D hearts. Importantly, MR16-1 completely prevented ventricular fibrosis in S16D hearts (**Figures 5E and 5F**). To confirm the fact that IL-6 signaling was inhibited by MR16-1 in S16D hearts, cardiac fibroblasts were isolated, and P-STAT3/total STAT3 levels were assessed through

FIGURE 5 MR16-1 Treatment Attenuates Fibrosis and Improves Cardiac Function

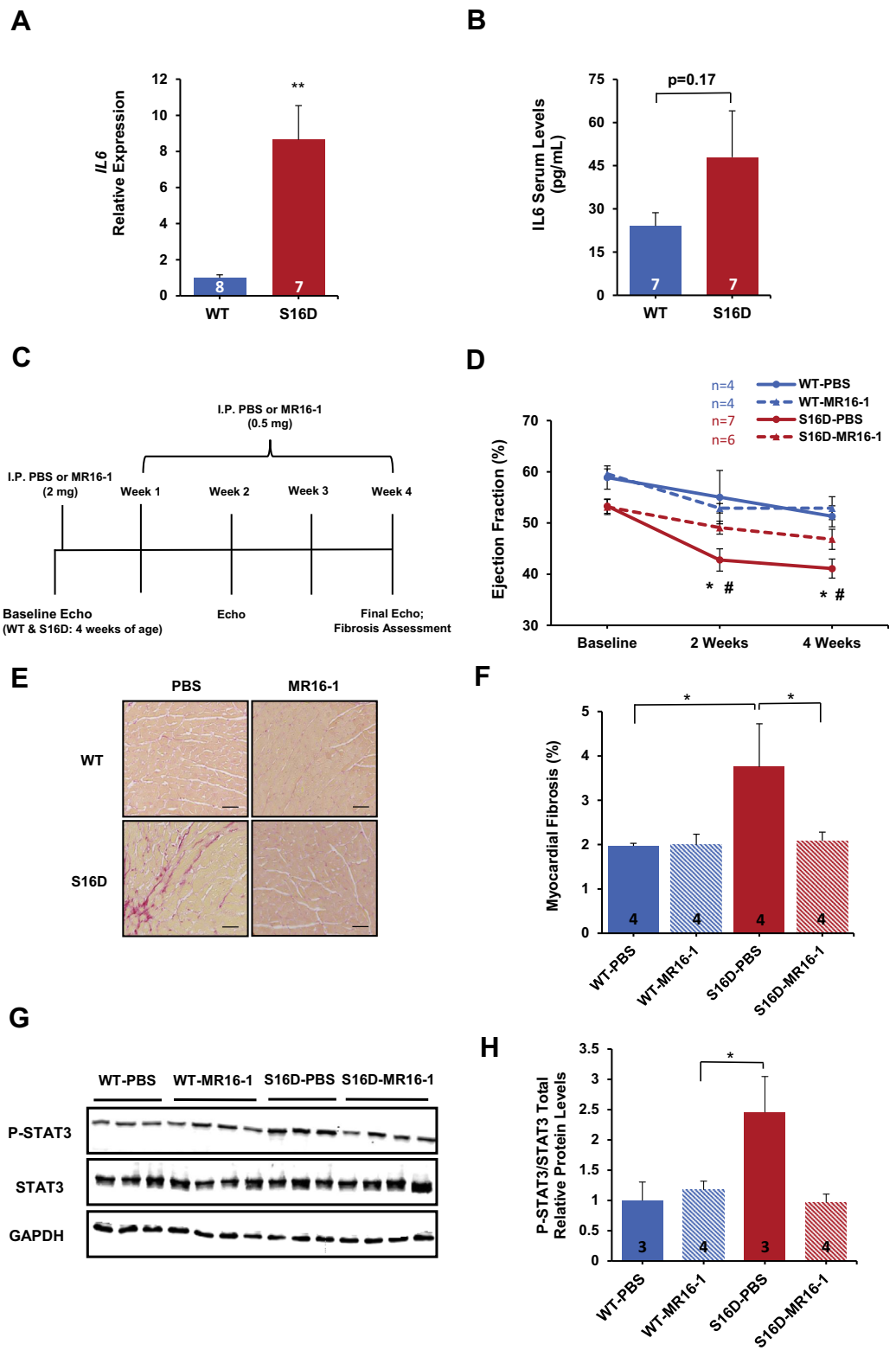

Continued on the next page

Western blotting. Indeed, fibroblasts isolated from S16D-PBS-treated hearts showed an increase in P-STAT3 levels, which was abrogated by treatment with the MR16-1 antibody. These results suggested that upregulation of IL-6 contributes to the acceleration of cardiac fibrosis and dysfunction in S16D TG mice.

DISCUSSION

The current study reveals a novel pro-fibrotic role of phosphorylated Hsp20 (S16D-Hsp20) through regulation of myocyte-synthesized IL-6 and subsequent paracrine activation of myofibroblast differentiation. These insights were acquired through characterization of a TG mouse model with cardiac-specific overexpression of constitutively phosphorylated Hsp20 (S16D-Hsp20), which demonstrated fibrotic ventricular remodeling at an early age.

Cardiac fibroblasts are essential for maintaining normal cardiac function, as they provide a structural network for cardiomyocytes, distribute mechanical forces through the cardiac tissue, and mediate electric conduction (19). In response to pathological stimuli, these cells undergo a transition to a myofibroblast phenotype, which can secrete elevated levels of extracellular matrix (ECM) proteins aimed at maintaining the structural integrity of the heart (19). However, a sustained fibrotic response can lead to reduced ventricular compliance, cardiac dysfunction, and ultimately heart failure (19). There are 2 distinct types of cardiac fibrosis: 1) reactive interstitial fibrosis, which is an expansion of the ECM in the absence of cardiomyocyte loss; and 2) replacement fibrosis, which results in extensive cardiomyocyte death (27). In the present study, S16D was associated with extensive cardiac interstitial fibrosis as early as 2 months of age, without evidence of cardiomyocyte apoptosis. Thus, it appears that cell death was not the initial driving force behind the early interstitial fibrosis, consistent with previous in vitro findings indicating that S16D renders cardiomyocyte protection from apoptosis (9).

The fine communication between cardiac myocytes and fibroblasts plays a key role in cardiac remodeling mediated by paracrine factors (21). These factors include numerous cytokines such as TGF-β1, IL-6, IL-1β, and TNF-α, which have been implicated in fibroblast proliferation and myofibroblast activation (21,22,26). Findings of the present study indicate that the S16D overexpression in cardiomyocytes also activated myofibroblast differentiation in a paracrine fashion. This was shown by enhanced proliferation and upregulation in expression of collagens, cytokines, and αSMA stress fibers. The pro-fibrotic effects were specific to S16D, as medium from Ad.S16A (constitutively dephosphorylated) cardiomyocytes had no effects. Further assessment of the S16D-infected cardiomyocytes indicated the transcriptional upregulation of IL-6. These effects were specific to IL-6, as there were no alterations in gene expression of other cytokines. Accordingly, secretion of IL-6 from the cardiomyocytes contributed to activation of fibroblasts to myofibroblasts, as shown by a reduction of the pro-fibrotic effects when using the IL-6 neutralizing antibody.

IL-6 is a pleiotropic cytokine whose expression in the heart has received particular interest, as its circulatory and intracardiac levels are elevated in congestive heart failure and are powerful predictors of LV remodeling (28,29). IL-6 signaling occurs through the transcription factor STAT3, which, upon phosphorylation at tyrosine 705, translocates to the nucleus and activates a broad array of target genes (25). In the cardiac fibroblast, STAT3 activation has been demonstrated to promote fibroblast proliferation in addition to synthesis of ECM proteins (25). Results of the present study show that S16D overexpression in cardiomyocytes promotes IL-6 secretion, which subsequently activates nuclear

FIGURE 5 Continued

(A) Quantification of *IL-6* gene expression levels in S16D hearts and WT control hearts. Values were normalized to those of the internal control GAPDH and expressed as fold-changes relative to those of WT mice. **(B)** Quantification of *IL-6* serum levels in S16D and WT control mice was determined by using an ELISA assay. **(C)** Schematic presentation of S16D and WT control mice treated with MR16-1 or PBS (control) starting at 1 month of age. Following the baseline echocardiographic assessment, mice were injected with 2 mg/body weight MR16-1 or PBS. Subsequently, mice received 0.5 mg/body per week (2 injections of 0.25 mg/body) during weeks 1, 2, and 3. **(D)** Left ventricular ejection fraction at baseline and at 2 and 4 weeks; *$p < 0.05$ versus WT-PBS; #$p < 0.05$ versus S16D-MR16-1. **(E)** Representative images (original magnification: ×20) of Picrosirius **red** staining following 4 weeks of treatment; scale bar: 50 μm. **(F)** Quantification of percent of ventricular fibrosis (fibrotic area/total ventricular area). **(G)** Representative Western blots and **(H)** quantification of P-STAT3 (Y705)/total STAT3 protein levels of the indicated groups. Values are fold-changes relative to those of WT-PBS. The number of samples (n) per group is indicated on the bar graphs. GAPDH = glyceraldehyde 3-phosphate dehydrogenase; I.P. PBS = intraperitoneal phosphate buffered saline; P-STAT3 = phosphorylated STAT3; other abbreviations as in Figures 3 and 4.

translocation of phosphorylated STAT3 (P-STAT3) in fibroblasts and increased expression of collagen and cytokines. Importantly, addition of the IL-6 neutralizing antibody reduced the P-STAT3 and attenuated the pro-fibrotic effects of S16D. Thus, IL-6/STAT3 signaling appears to mediate the paracrine effects of the S16D cardiomyocyte.

The ex vivo findings described previously led to the hypothesis that IL-6 may contribute to cardiac remodeling and dysfunction observed in the S16D mouse model. Indeed, cardiac gene expression as well as serum levels of IL-6 were elevated in S16D hearts as early as 2 months of age. To confirm the contribution of IL-6 in cardiac remodeling and dysfunction, S16D mice were treated with the selective IL-6 receptor antagonist monoclonal antibody MR16-1. Isolated cardiac fibroblasts revealed that STAT3 signaling was elevated in the nontreated S16D hearts, although this effect was abolished by treatment with the MR16-1 antibody. Accordingly, MR16-1 prevented the development of interstitial fibrosis and preserved EF. However, MR16-1 treatment had no effects on the observed alterations of LV chamber dilation, cardiomyocyte hypertrophy, or remodeling markers, as these parameters were similar to those in nontreated S16D mice. Taken together, IL-6/STAT3 signaling appears to contribute to fibroblast activation and the resultant development of interstitial fibrosis in S16D hearts. Nonetheless, the lack of protection against remodeling in the MR16-1-treated S16D hearts indicates that these pathological alterations are driven by additional factors other than the IL-6/STAT3 pathway.

These results suggest that chronic phosphorylation of Hsp20 is associated with ventricular remodeling and dysfunction, partially mediated through the pro-fibrotic action of cardiomyocyte-synthesized IL-6. Thus, targeting the levels of S16D-Hsp20 in human heart failure may represent an effective strategy for limiting fibrotic remodeling.

STUDY LIMITATIONS. Although the current findings highlight the significance of chronic Hsp20 phosphorylation in cardiac fibrosis, use of the TG mouse model in this study may be criticized as limiting. Generation of a gene-targeted knock-in mouse model would have been a more elegant model for examining the significance of Hsp20 phosphorylation in vivo. However, transgenesis was chosen because the aim was to overexpress S16D-Hsp20 at levels similar to those observed in human heart failure. The authors recognize that additional mechanisms might have contributed to cardiac remodeling in the S16D hearts. For the purpose of this study, the authors focused specifically on the regulation of IL-6 in the cardiomyocyte and its subsequent paracrine effects on the cardiac fibroblast.

CONCLUSIONS

Ex vivo and in vivo studies have revealed a novel role for phosphorylated Hsp20 in the heart involving upregulation of IL-6 in the cardiomyocyte and the associated paracrine activation of cardiac fibroblasts. Thus, hyperphosphorylation of Hsp20 in human failing hearts coupled with findings from the current study suggest that it may play a role in pathological remodeling and, thus, may provide a new therapeutic opportunity.

ACKNOWLEDGEMENTS The authors thank the Live Microscopy Core in the Department of Pharmacology and Systems Physiology, University of Cincinnati, for providing technical assistance with confocal microscopy.

ADDRESS FOR CORRESPONDENCE: Dr. Evangelia G. Kranias, Department of Pharmacology and Systems Physiology, University of Cincinnati College of Medicine, 231 Albert Sabin Way, Cincinnati, Ohio 45267-0575. E-mail: KRANIAEG@ucmail.uc.edu.

PERSPECTIVES

COMPETENCY IN MEDICAL KNOWLEDGE: Cardiac fibrosis, characterized by excessive deposition of extracellular matrix proteins, is a key component in ventricular remodeling and the pathophysiology of heart failure. Crosstalk between cardiomyocytes and cardiac fibroblasts through paracrine factors has emerged as a factor in this remodeling process. However, there is a need to gain further insights into this apparent cardiac myocyte/fibroblast communication to prevent heart failure progression. Findings from the present study demonstrate that phosphorylated Hsp20 may act as a regulator in paracrine-induced fibrotic remodeling.

TRANSLATIONAL OUTLOOK: Hsp20 phosphorylation is chronically elevated in human and experimental heart failure. Explorations in the relevance of these increases in a murine model indicates that they associate with fibrotic ventricular remodeling and contractile dysfunction. Therefore, Hsp20 may serve as a novel therapeutic target in heart failure.

REFERENCES

1. Savarese G, Lund LH. Global public health burden of heart failure. Card Fail Rev 2017;3:7–11.

2. Lohse MJ, Engelhardt S, Eschenhagen T. What is the role of beta-adrenergic signaling in heart failure? Circ Res 2003;93:896–906.

3. Lou Q, Janardhan A, Efimov IR. Remodeling of calcium handling in human heart failure. Adv Exp Med Biol 2012;740:1145–74.

4. Nicolaou P, Hajjar RJ, Kranias EG. Role of protein phosphatase-1 inhibitor-1 in cardiac physiology and pathophysiology. J Mol Cell Cardiol 2009;47:365–71.

5. Kappé G, Franck E, Verschuure P, Boelens WC, Leunissen JA, De jong WW. The human genome encodes 10 alpha-crystallin-related small heat shock proteins: HspB1-10. Cell Stress Chaperones 2003;8:53–61.

6. Fan GC, Chu G, Kranias EG. Hsp20 and its cardioprotection. Trends Cardiovasc Med 2005;15:138–41.

7. Qian J, Ren X, Wang X, et al. Blockade of Hsp20 phosphorylation exacerbates cardiac ischemia/reperfusion injury by suppressed autophagy and increased cell death. Circ Res 2009;105:1223–31.

8. Fan GC, Kranias EG. Small heat shock protein 20 (HspB6) in cardiac hypertrophy and failure. J Mol Cell Cardiol 2011;51:574–7.

9. Fan GC, Chu G, Mitton B, et al. Small heat-shock protein Hsp20 phosphorylation inhibits beta-agonist-induced cardiac apoptosis. Circ Res 2004;94:1474–82.

10. Fan GC, Yuan Q, Song G, et al. Small heat-shock protein Hsp20 attenuates beta-agonist-mediated cardiac remodeling through apoptosis signal-regulating kinase 1. Circ Res 2006;99:1233–42.

11. Fan GC, Zhou X, Wang X, et al. Heat shock protein 20 interacting with phosphorylated Akt reduces doxorubicin-triggered oxidative stress and cardiotoxicity. Circ Res 2008;103:1270–9.

12. Fan GC, Ren X, Qian J, et al. Novel cardioprotective role of a small heat-shock protein, Hsp20, against ischemia/reperfusion injury. Circulation 2005;111:1792–9.

13. Chu G, Egnaczyk GF, Zhao W, et al. Phosphoproteome analysis of cardiomyocytes subjected to beta-adrenergic stimulation: identification and characterization of a cardiac heat shock protein p20. Circ Res 2004;94:184–93.

14. Travers JG, Kamal FA, Valiente-alandi I, et al. Pharmacological and activated fibroblast targeting of Gβγ-GRK2 after myocardial ischemia attenuates heart failure progression. J Am Coll Cardiol 2017;70:958–71.

15. Fredj S, Bescond J, Louault C, Delwail A, Lecron JC, Potreau D. Role of interleukin-6 in cardiomyocyte/cardiac fibroblast interactions during myocyte hypertrophy and fibroblast proliferation. J Cell Physiol 2005;204:428–36.

16. Ueda O, Tateishi H, Higuchi Y, et al. Novel genetically-humanized mouse model established to evaluate efficacy of therapeutic agents to human interleukin-6 receptor. Sci Rep 2013;3:1196.

17. Hartman MH, Vreeswijk-baudoin I, Groot HE, et al. Inhibition of interleukin-6 receptor in a murine model of myocardial ischemia-reperfusion. PLoS One 2016;11:e0167195.

18. Liu T, Song D, Dong J, et al. Current understanding of the pathophysiology of myocardial fibrosis and its quantitative assessment in heart failure. Front Physiol 2017;8:238.

19. Travers JG, Kamal FA, Robbins J, Yutzey KE, Blaxall BC. Cardiac fibrosis: the fibroblast awakens. Circ Res 2016;118:1021–40.

20. Martin ML, Blaxall BC. Cardiac intercellular communication: are myocytes and fibroblasts fair-weather friends? J Cardiovasc Transl Res 2012;5:768–82.

21. Pellman J, Zhang J, Sheikh F. Myocyte-fibroblast communication in cardiac fibrosis and arrhythmias: mechanisms and model systems. J Mol Cell Cardiol 2016;94:22–31.

22. Talman V, Ruskoaho H. Cardiac fibrosis in myocardial infarction-from repair and remodeling to regeneration. Cell Tissue Res 2016;365:563–81.

23. Aoyagi T, Matsui T. The cardiomyocyte as a source of cytokines in cardiac injury. J Cell Sci Ther 2011;2012(S5).

24. Porter KE, Turner NA. Cardiac fibroblasts: at the heart of myocardial remodeling. Pharmacol Ther 2009;123:255–78.

25. Haghikia A, Ricke-Hoch M, Stapel B, Gorst I, Hilfiker-Kleiner D. STAT3, a key regulator of cell-to-cell communication in the heart. Cardiovasc Res 2014;102:281–9.

26. Meléndez GC, Mclarty JL, Levick SP, Du Y, Janicki JS, Brower GL. Interleukin 6 mediates myocardial fibrosis, concentric hypertrophy, and diastolic dysfunction in rats. Hypertension 2010;56:225–31.

27. Piek A, De Boer RA, Silljé HH. The fibrosis-cell death axis in heart failure. Heart Fail Rev 2016;21:199–211.

28. Kanda T, Takahashi T. Interleukin-6 and cardiovascular diseases. Jpn Heart J 2004;45:183–93.

29. Kobara M, Noda K, Kitamura M, et al. Antibody against interleukin-6 receptor attenuates left ventricular remodelling after myocardial infarction in mice. Cardiovasc Res 2010;87:424–30.

KEY WORDS fibroblast, heart failure, Hsp20, IL-6, remodeling

APPENDIX For an expanded methods section and supplemental figures, please see the online version of this paper.